Articles

Factors Affecting the Magnitude of the Metal-Insulator Transition Temperature in AMo_4O_6 (A=K, Sn)

Dongwoon Jung,* Kwangsik Choi, and Sungjin Kim†,*

Department of Chemistry and Institute of Basic Natural Science, Wonkwang University, Iksan, Jeonbuk 570-749, Korea
†Department of Chemistry, Ewha University, Seoul 120-750, Korea
Received January 30, 2004

A low-dimensional metal frequently exhibits a metal-insulator transition through a charge-density-wave (CDW) or a spin-density-wave (SDW) which accompany it's structural changes. The transition temperature is thought to be determined by the amount of energy produced during the transition process and the softness of the original structure. AMo_4O_6 (A=K, Sn) are known to be quasi-one dimensional metals which exhibit metal-insulator transitions. The difference of the transition temperatures between KMo_4O_6 and $SnMo_4O_6$ (A=K, Sn) is examined by investigating their electronic and structural properties. Fermi surface nesting area and the lattice softness are the governing factors to determine the metal-insulator transition temperature in AMo_4O_6 compounds.

Key Words : Molybdenum oxide, Charge density wave, Electronic structure

Introduction

During the last decade, the metal-metal bonded ternery molybdenum oxide systems KMo_4O_6 [1] and $SnMo_4O_6$ [2] were successfully synthesized and characterized. These compounds are structurally similar in that they are low-valent molybdenum oxides containing Mo_6O_{12} type octahedral clusters condensed by sharing trans-edges to form infinite chains, but are different in that either K^+ or Sn^{2+} cation is filled in a square channel which is constructed by four adjacent perpendicularly bridged chains. Since all chains are extended along the crystallographic c-direction, AMo_4O_6(A=K, Sn) compounds are supposed to show one-dimensional (1D) electronic property.[3] On the basis of the assumption that the unique role of the cations are electron donors, the electronic structures of the electron withdrawing part (*i.e.*, $Mo_4O_6^{n-}$) should be different depending upon the charge of a cation.

Low dimensional metals often possess electronic instabilities toward a metal-insulator transition, which occur when the Fermi surface of their partially filled bands are nested.[4,5] In general, the Fermi surface of a one-dimensional metal is well nested, the 1D metal frequently shows a metal-insulator transition. The metal-insulator transition can occur either at lower temperature or at higher temperature depending upon the lattice softness and the amount of energy gain during the transition process which is related to the nested area. It is necessary, therefore, to investigate structural and electronic properties of low-dimensional metals in order to understand their different transition temperatures. In the present work, we report the factors affecting the magnitude of the metal-insulator transition temperature in AMo_4O_6 (A=K, Sn) by examining the electronic structure of this compound on the basis of the crystal structure.

Crystallographic Data

The crystal structures of KMo_4O_6 and $SnMo_4O_6$ are almost similar to each other except the difference between the oxidation state and the size of the cation.[1,2] The perspective view of the structure of $SnMo_4O_6$ along the crystallographic c-direction which is similar to that of KMo_4O_6, is shown in Figure 1. It is clear from the figure that Mo-Mo and Mo-O bonds construct a rectangular unit. In a rectangular unit, two Mo atoms (Mo-1) on long sides of a

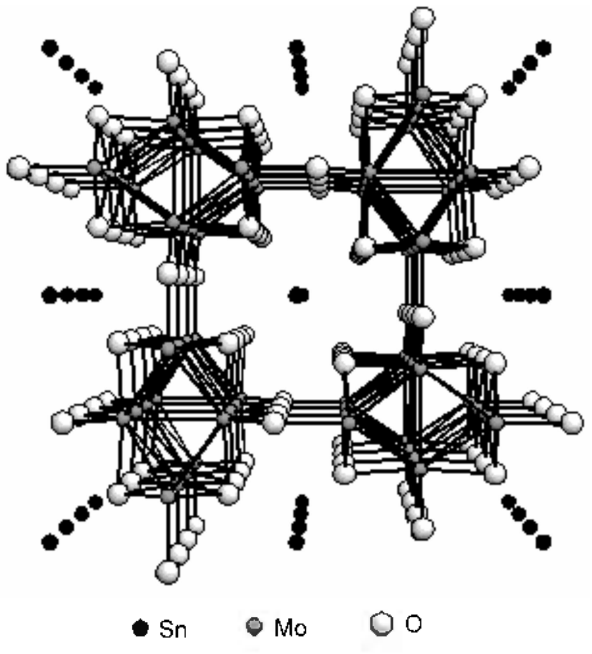

Figure 1. The perspective view of the structure of $SnMo_4O_6$.

Table 1. Crystal Data and Structure Refinement for $SnMo_4O_6$

empirical formula	$SnMo_4O_6$
formula weight	422.57
temperature, K	293(2)
wavelength, Å	0.71073
crystal system	tetragonal
space group	P4/mbm
unit cell dimension, Å	a = 9.5804(9) b = 9.5804(9) c = 2.8436(4)
volume, Å^3	261.00(5)
Z	2
density (calculated)	5.398 mg/cm^3
absorption coefficient	4.727 mm^{-1}
θ range for data collection	3.01°- 24.85°

Table 2. Crystal Data and Structure Refinement for KMo_4O_6

empirical formula	KMo_4O_6
formula weight	518.86
temperature, K	296
wavelength, Å	0.71069
crystal system	tetragonal
space group	$P\bar{4}$
unit cell dimension, Å	a = 9.636(1) b = 9.636(1) c = 2.879(1)
volume, Å^3	267.32(1)
Z	2
density (calculated)	6.44 mg/cm^3
θ range for data collection	4°-84°

rectangle are positioned behind by c/2 compared with those (Mo-2) on short sides of the rectangle. When the next pair of Mo-2 atoms are added to the four given Mo-Mo cluster in a rectangular unit, then one can easily construct a distorted Mo_6 octahedron, which is edge-shared with the next Mo_6 along the c-direction. Four rectangular units are bonded through bridging oxygens to construct a channel in which the cations sit. Consequently, the Mo_6 octahedra are continuously connected along the c-direction through Mo-Mo bonds, while those are connected along the a- and b-directions through bridging oxygens. Crystallographic data

Table 3. Atomic coordinates ($\times 10^{-4}$) and equivalent isotropic displacement parameters (Å$^2\times 10^{-3}$) for $SnMo_4O_6$

	x	y	z	U (eq)
Sn(1)	0	0	0	9(1)
Mo(1)	3979(1)	1021(1)	0	4(1)
Mo(2)	6446(1)	1446(1)	-5000	9(1)
O(1)	2927(5)	2073(5)	-5000	7(2)
O(2)	2359(5)	-412(5)	0	10(2)

U(eq) is defined as one third of the trace of the orthogonalized U_{ij} tensor.

Table 4. Atomic coordinates ($\times 10^{-4}$) and equivalent isotropic displacement parameters (Å$^2\times 10^{-3}$) for KMo_4O_6

	x	y	z	U (eq)
K(1)	0.	0.	0.5	1.31(3)
K(2)	0.5	0.5	0.5	1.29(3)
Mo(1)	0.60105(4)	0.10101(4)	-0.0002	0.347(4)
Mo(2)	0.14276(4)	0.64262(4)	0.5069(3)	0.564(5)
O(1)	0.2052(4)	0.2942(4)	0.494(3)	0.62(4)
O(2)	0.2431(4)	0.0461(4)	-0.001(4)	0.63(4)
O(3)	0.4545(4)	0.2568(4)	-0.010(4)	0.65(4)

Table 5. Bond lengths [Å] and angles [deg] for $SnMo_4O_6$

Bond	
Sn(1)-O(2)	2.294(5)
Sn(1)-Sn(1)	2.8436(4)
Mo(1)-O(1)	2.014(5)
Mo(1)-O(2)	2.072(5)
Mo(1)-Mo(1)	2.765(2)
Mo(1)-Mo(2)	2.7879(8)
Mo(1)-Mo(1)#5	2.8436(4)
Mo(2)-O(1)#9	2.006(7)
Mo(2)-O(2)#7	2.077(4)
Mo(2)-Mo(1)#8	2.7879(8)
Mo(2)-Mo(1)#5	2.7879(8)
Mo(2)-Mo(1)#7	2.7879(8)
Mo(2)-Mo(2)#4	2.8436(4)
Mo(2)-Mo(2)#5	2.8436(4)
O(2)#1-Sn(1)-O(2)#2	90.0
O(2)#2-Sn(1)-O(2)	180.0
O(2)#1-Sn(1)-Sn(1)#4	90.0
Sn(1)#4-Sn(1)-Sn(1)#5	180.0
O(2)-Mo(1)-Mo(1)#4	90.0
Mo(1)#7-Mo(1)-Mo(1)#4	90.0

of KMo_4O_6 and $SnMo_4O_6$ are given in Table 1 and Table 2, respectively. Cell parameters and fractional coordinates of atoms of KMo_4O_6 and $SnMo_4O_6$ for the calculation are given in Table 3 and Table 4, respectively. The cation-oxygen distance is shorter in $SnMo_4O_6$ (*i.e.*, Sn-O; 2.294 Å) than in KMo_4O_6 (*i.e.*, K-O; 2.770 Å). The Mo-Mo bond distances are also slightly shorter in $SnMo_4O_6$ (*i.e.*, 2.765 Å, 2.788 Å and 2.843 Å) than those in KMo_4O_6 (*i.e.*, 2.754 Å, 2.774 Å, 2.794 Å and 2.879 Å), which results in the displacements of the bridging oxygen atoms closer toward the central cation. The selected bond distances and angles in both compounds are listed in Tables 5 and 6, respectively.

Electrical resistivity data. The electrical resistivity data along the crystallographic c-direction of $SnMo_4O_6$ and KMo_4O_6 as a function of temperature are shown in Figures 2 and 3, respectively. It is clear from the resistivity data that $SnMo_4O_6$ and KMo_4O_6 show metal-insulator transitions at 50 K and 120 K,[2] respectively. The difference in the metal-insulator transition temperature in $SnMo_4O_6$ and KMo_4O_6 will be analyzed by examining the structural and electronic properties of both compounds. The resistivity along the c-

Table 6. Selected bond lengths [Å] for KMo_4O_6

Bond	
K(1)-O(2)	2.783(7) [4 ×]
K(2)-O(2)	2.787(7) [4 ×]
K(2)-O(3)	2.800(7) [4 ×]
K(2)-O(3)	2.770(7) [4 ×]
Mo(1)-O(1)	2.013(6)
Mo(1)-O(1)	2.037(6)
Mo(1)-O(2)	2.066(4)
Mo(1)-O(3)	2.061(4)
Mo(2)-O(1)	2.069(4)
Mo(2)-O(2)	2.049(9)
Mo(2)-O(2)	2.027(9)
Mo(2)-O(3)	2.033(9)
Mo(2)-O(3)	2.045(9)
Mo(1)-Mo(1)	2.879(1) [2 ×]
Mo(1)-Mo(1)	2.754(1)
Mo(1)-Mo(2)	2.794(1) [2 ×]
Mo(1)-Mo(2)	2.774(1) [2 ×]
Mo(1)-Mo(2)	2.793(1) [2 ×]
Mo(1)-Mo(2)	2.773(1) [2 ×]
Mo(2)-Mo(2)	2.879(1) [2 ×]

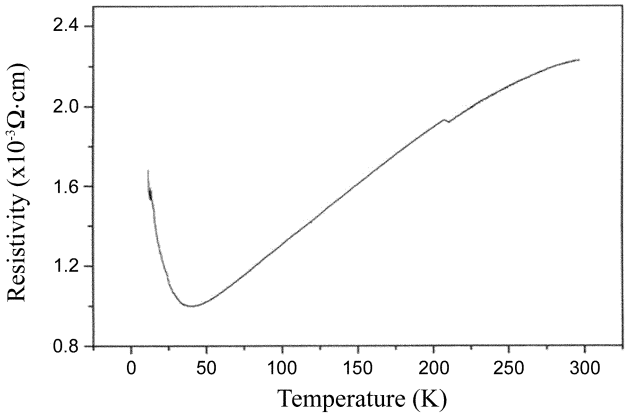

Figure 2. Electrical resistivity (ρ) of $SnMo_4O_6$ as a function of temperature (T).

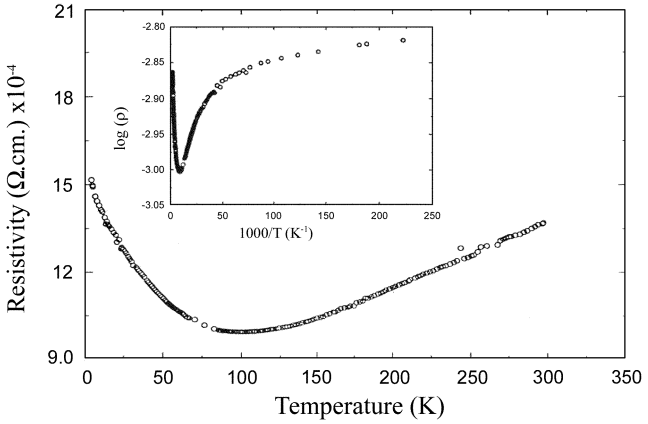

Figure 3. Electrical resistivity (ρ) of KMo_4O_6 as a function of temperature (T). The inset shows the relationship between log(ρ) versus 1/T.

Table 7. Atomic Parameters used in EHTB Calculations[a]: Valence orbital Ionization Potential H_{ii} (eV) and Exponent of the Slater-type Orbital ζ

atom	orbital	H_{ii}	ζ_1 (c_1)	ζ_2 (c_2)
Mo	4d	-10.50	4.54 (0.5899)	1.90 (0.5899)
	5s	-8.34	1.96	
	5p	-5.24	1.90	
O	2s	-32.3	2.275	
	2p	-14.8	2.275	

[a]Parameters are collected from the following data: (a) Clementi, E.; Roetti, C. *Atomic Data Nuclear Data Tables* **1974**, *14*, 177. (b) McLean, A. D.; McLean, R. S. *Atomic Data Nuclear Data Tables* **1981**, *26*, 197. (c) Richardson, J. W.; Blackman, M. J.; Ranochak, J. E. *J. Chem. Phys.* **1973**, *58*, 3010.

axis for $SnMo_4O_6$ and KMo_4O_6 at room temperature are about 2.2×10^{-3} Ω·cm and 1.3×10^{-3} Ω·cm, respectively.

Electronic structure calculations. The electronic structures of $SnMo_4O_6$ and KMo_4O_6 were investigated by performing tight-binding band electronic structure calculations based upon the extended Huckel method.[6,7] The PC version of CAESAR program was used for the calculations. Atomic parameters adopted in the calculations are shown in Table 7.

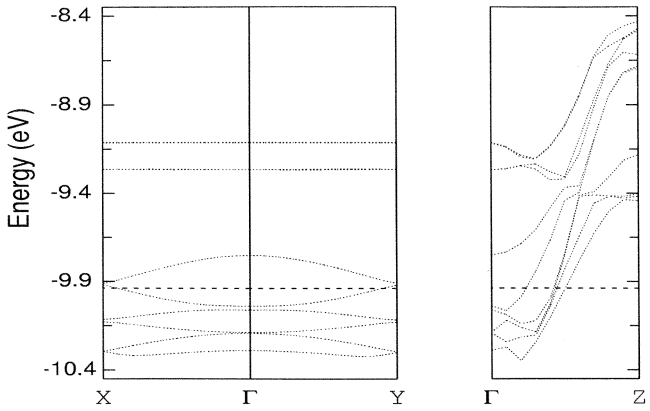

Figure 4. Band dispersions calculated for $SnMo_4O_6$ where Γ, X, Y, and Z represent (0.0.0), (π/a.0.0), (0.π/b, 0) and (0.0.π/c). The dashed lines refer to the Fermi energy.

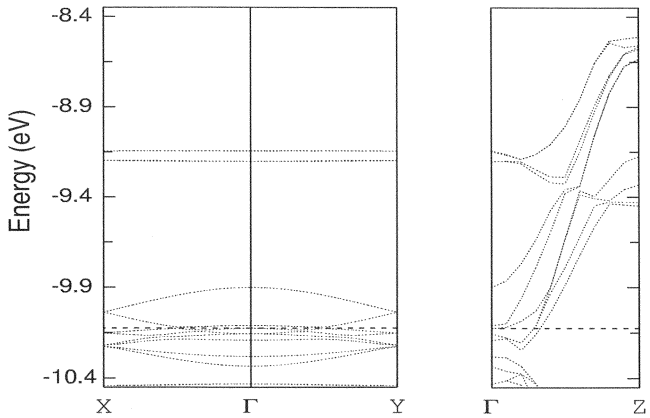

Figure 5. Band dispersions calculated for KMo_4O_6.

Results and Discussion

In each unit cell, there are two sets of AMo_4O_6 since Z=2. $(Mo_8O_{12})^{n-}$ are, therefore, chosen as a unit for electronic structure calculations for both compounds. Band dispersions calculated for $(Mo_8O_{12})^{0-}$ units of $SnMo_4O_6$ and KMo_4O_6 are shown in Figure 4 and 5, respectively, where Γ, X, Y, and Z represent (0,0,0), (π/a,0,0), (0,π/b,0) and (0,0,π/c) in the reciprocal lattice, respectively. The dispersion curves along the a^*-direction is exactly same to that along the b^*-direction in both compounds since the crystals are tetragonal. The bands are strongly dispersive along the c^*-direction while those along the a^*- and b^*-directions are weakly dispersive. The band dispersions clearly tell us that $SnMo_4O_6$ and KMo_4O_6 are said to be a quasi-one-dimensional metal. Fermi level of $SnMo_4O_6$ is higher than that of KMo_4O_6 since Sn contributes more electrons to Mo_4O_6 than K. Depending upon the position of Fermi energy, five bands are cut by Fermi energy in $SnMo_4O_6$, while four bands are cut in KMo_4O_6.

Fermi surfaces associated with the partially filled band dispersions of $SnMo_4O_6$ and KMo_4O_6 are shown in Figures 6 and 7, respectively. In $SnMo_4O_6$, the Fermi surfaces associated with the lowest four bands [see Figures 6(a)-6(d)] are open along the a^*- and b^*-directions while they are closed along the c^*-direction, which means that the electrical conductivity arises only along the c-axis. On the other hand, the Fermi surface associated with the highest band [see Figure 6(e)] shows 3-dimensional nature. Consequently, electrons moving along the c^*-direction dominate to arise the

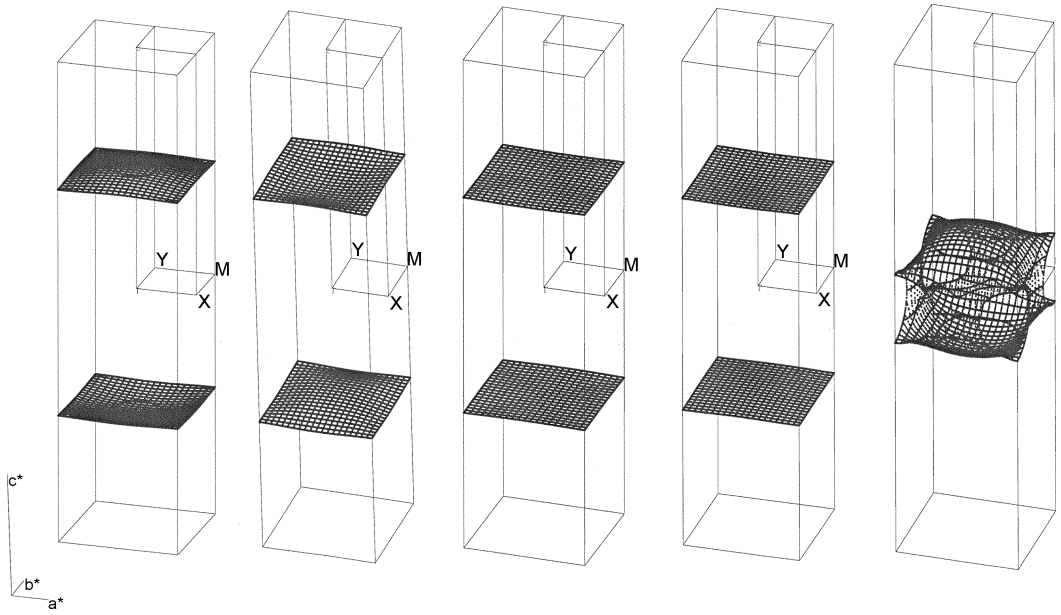

Figure 6. Fermi surface associated with the five partially filled band dispersions of $SnMo_4O_6$.

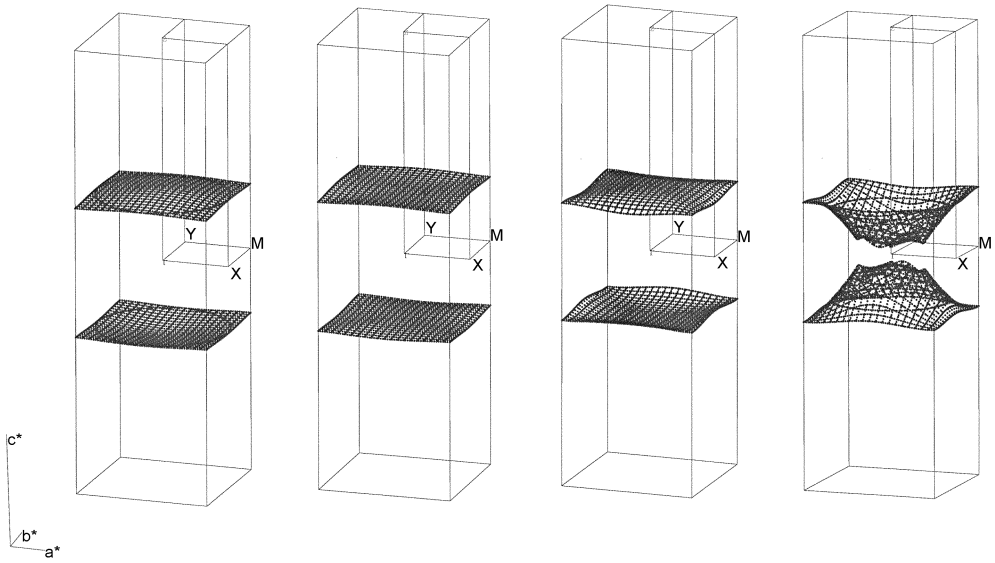

Figure 7. Fermi surfaces associated with the four partially filled band dispersions of KMo_4O_6.

metallic property of the compound. Since conductivity of a metal is proportional to the number of electrons per unit volume, that along the c^*-direction is much higher than those along the other two directions as discussed earlier, and hence $SnMo_4O_6$ possesses 1D character. Similarly to those in $SnMo_4O_6$, the 1D Fermi surfaces associated with the lowest two bands of KMo_4O_6 are shown in Figures 7(a), 7(b) and 7(c), which are open along the a^*- and b^*-directions. In addition, the Fermi surface associated with the highest band [see Figure 7(d)] shows 3-dimensional nature. Generally the 1D Fermi surface is well nested as one can find in the figures. There are four and three 1D Fermi surfaces in $SnMo_4O_6$ and KMo_4O_6, respectively. In addition, the shape of the Fermi surfaces is flatter in those of $SnMo_4O_6$ than in those of KMo_4O_6. The nested area is, therefore, larger in $SnMo_4O_6$ than in KMo_4O_6. A metallic state may not be stable when its Fermi surface is nested, and is susceptible to become an insulating state when temperature is lowered. The metal-insulator(M-I) transition leads to a charge density wave (CDW) state or a spin density wave (SDW) state.[8-10] Let us discuss why a Fermi surface nesting is important in introducing an M-I transition by investigating the orbital mixing between an occupied and unoccupied levels.[10] For a 1D metal, an occupied wave vector k and a unoccupied wave vector k' form an occupied orbital $\Phi(k)$ and a unoccupied orbital $\Phi(k')$, respectively. An orbital mixing between $\Phi(k)$ and $\Phi(k')$ produces new orbitals $\Psi(k)$ and $\Psi(k')$.

$$\Psi(k) \propto \Phi(k) + \gamma\Phi(k')$$
$$\Psi(k') \propto -\gamma\Phi(k) + \Phi(k')$$

where γ is a mixing coeffiecient. The extent of the orbital mixing is determined by the energy difference between the original orbitals $\Phi(k)$ and $\Phi(k')$. At the Fermi level, by definition, two orbitals $\Phi(k)$ and $\Phi(k')$ are degenerate. Therefore, the orbital mixing between them is significant and so is the interaction energy $\langle\Phi(k)|H'|\Phi(k')\rangle$. When a Fermi surface is nested by a vector q, the orbital mixing can be performed for all wave vectors in the nested region of the First Brillouin Zone (FBZ), thereby leading to the sets of new orbitals $\{\Phi(k)\}$ and $\{\Phi(k)\}$ differing in their wave vectors by $q = k-k'$. As the nesting area is large, therefore, the amount of orbital mixing is large and so is the extent of interaction energy. This large amount of energy becomes the driving force to change the structure which leads to an M-I transition even at low temperature. Consequently, the M-I transition temperature in $SnMo_4O_6$ is lower than that in KMo_4O_6. The unnested Fermi surface associated with the highest bands in both compounds may exhibit some metallic character for the compounds even after the M-I transition. But when the change in the crystal structure caused by the M-I transition associated from the nested Fermi surfaces is strong enough, the compound after the M-I transition may not have partially filled bands.

As the interatomic distance becomes longer, the overlap between atoms would eventually become smaller, and all bands, even the partially filled conduction bands, would become narrower. As the conduction band become narrower, the velocity of the electrons in it would diminish and the conductivity of the metal would drop to zero which means that it becomes an insulator.[12] In $SnMo_4O_6$ and KMo_4O_6, conduction arises along the c-direction where Mo-Mo and Mo-O bonds are constructed. As mentioned in crystallographic data, Mo-Mo and Mo-O distances are shorter in $SnMo_4O_6$ than in KMo_4O_6. So the overlap in Mo-Mo and Mo-O bonds is smaller in KMo_4O_6 than in $SnMo_4O_6$. In addition, the velocity of electrons is a function of temperature. In the long run, the metallic property is disappeared even at higher temperature and become an insulator in KMo_4O_6. The M-I transition appears, therefore, at higher temperature in KMo_4O_6 than in $SnMo_4O_6$ as shown in the resistivity data. Low-dimensional metals frequently possess electronic instabilities toward an M-I transition or a metal-superconductor transition. Whatever it shows, a phase transition occurs at certain temperature. It means that the position of the transition temperature (T_c) is affected by the similar factors. In the metal-superconducting transition, the T_c strongly depends on the lattice softness according to the BCS theory.[13] The compound having softer lattice exhibits higher T_c. The lattice of KMo_4O_6 is softer than that of $SnMo_4O_6$, as one can find in the bond distances. Thus, the higher M-I transition temperature in KMo_4O_6 is also reasonable from the view point of lattice softness.

Conclusions

KMo_4O_6 and $SnMo_4O_6$ are quasi-one dimensional metallic compounds at room temperature. Although they are isostructural, KMo_4O_6 and $SnMo_4O_6$ show the metal-insulator transition at 120 K and 50 K, respectively. The investigations on the structural and electronic properties of these compounds tell us that the difference of the M-I transition temperature is strongly governed by the Fermi surface nesting area and the lattice softness. The large area of Fermi surface nesting leads to an M-I transition even at low temperature. Therefore, the higher M-I transition temperature in KMo_4O_6 is well understood. In addition, Mo-Mo and Mo-O distances are shorter in $SnMo_4O_6$ than in KMo_4O_6. So the overlap in Mo-Mo and Mo-O bonds is smaller in KMo_4O_6. In addition, the velocity of electrons is a function of temperature. Therefore, the metallic property is disappeared even at higher temperature and become an insulator in KMo_4O_6. In the long run, the longer Mo-O and Mo-Mo bond distances make KMo_4O_6 lattice become softer, thereby leading to higher M-I transition temperature. As a result, the Fermi surface nesting area and lattice softness are the governing factors to determine the metal-insulator transition temperature in AMo_4O_6 compounds.

Acknowledgement. This work was financially supported by Wonkwang university in the program year of 2003.

References

1. Ramanujachary, K. V.; Greenblatt, M.; Jones, E. B.; McCarroll,

W. H. *J. Solid State Chem.* **1993**, *102*, 69.
2. Jung, D.; Lee, B.-H.; Kim, S.-J.; Kang, W. *Chem. Mater.* **2001**, *13*, 1625.
3. (a). Greenblatt, M.; Vincent, H.; Marezio, M. *Low-Dimensional Properties of Molybdenum Bronzes and Oxides*; Schlenker, C., Ed.; Kluwer publisher: 1989. (b) Kang, D.-B. *Bull. Korean Chem. Soc.* **1995**, *16*, 929.
4. Whangbo, M.-H.; Canadell, E. *Acc. Chem. Res.* **1989**, *22*, 375.
5. Wilson, J. A.; DiSalvo, F. J.; Mahajan, S. *Adv. Phys.* **1975**, *24*, 117.
6. Ammeter, J. H.; Bürgi, H.-B.; Thibeault, J.; Hoffmann, R. *J. Am. Chem. Soc.* **1978**, *100*, 3686.
7. Whangbo, M.-H.; Hoffmann, R. *J. Am. Chem. Soc.*, **1978**, *100*, 6093.
8. Whangbo, M.-H. *J. Chem. Phys.* **1979**, *70*, 4963.
9. Whangbo, M.-H. *J. Chem. Phys.* **1980**, *73*, 3854.
10. Whangbo, M.-H. *J. Chem. Phys.* **1981**, *75*, 4983.
11. Whangbo, M.-H. *Acc. Chem. Res.* **1983**, *16*, 95.
12. Ashcroft, N. W.; Mermin, N. D. *Solid State Physics*; Saunders College Publisher: Philadelphia, 1975; p 685.
13. McMillan, W. L. *Phys. Rev.* **1968**, *167*, 331.